

## Supplementary Information:

# Realizing high thermoelectric performance in GeTe through decreasing phase transition temperature *via* entropy engineering

Yuting Qiu,<sup>1</sup> Yang Jin,<sup>2</sup> Dongyang Wang,<sup>2</sup> Mengjia Guan,<sup>3</sup> Wenke He,<sup>2</sup> Shang Peng,<sup>4</sup>  
Ruiheng Liu, Xiang Gao,<sup>6\*</sup> Li-Dong Zhao<sup>2\*</sup>

<sup>1</sup> School of Beihang, Beihang University, Beijing 100191, China

<sup>2</sup>School of Materials Science and Engineering, Beihang University, Beijing 100191, China

<sup>3</sup>Key Laboratory for Ultrafine Materials of Ministry of Education, East China University of Science and Technology, Shanghai 200237, China

<sup>4</sup>School of Physics and Technology, Center for Electron Microscopy and MOE Key Laboratory of Artificial Micro- and Nano-Structures, Wuhan University, Wuhan 430072, China

<sup>5</sup>Shanghai Institute of Ceramics, Chinese Academy of Sciences, Shanghai 201899, China

<sup>6</sup>Center for High Pressure Science and Technology Advanced Research, Beijing 100094, China

**\*Correspondence to:** xiang.gao@hpstar.ac.cn (XG); zhaolidong@buaa.edu.cn (LDZ).

---

## EXPERIMENTAL:

**Structural characterization:** For all samples, the phase purity and crystal structure were examined by the powder x-ray diffraction (XRD) with Cu K $\alpha$  ( $\lambda = 1.5418 \text{ \AA}$ ) radiation. The morphology and homogeneity of samples were performed with scanning electron microscope (SEM, Zeiss Supra 55), which is equipped with an electron diffraction x-ray spectrometry (EDXS) for local chemical analysis (Inca, Oxford Instrument). Samples for scanning transmission electron microscopy (STEM) analysis were prepared using gentle ion milling (PIPS 691, Gatan) after mechanical thinning and precision polishing. Plasma cleaning (EC-52000IC, JEOL) was carried out to remove any residual surface contaminations before STEM analysis. High-angle annular dark-field (HAADF) imaging were carried out in an aberration-corrected microscope (ARM200F, JEOL) operated at 200 kV, using an inner detector angle of 72 mrad and a convergence semi-angle for the electron probe of 30 mrad.

**Hall measurements:** Hall coefficient ( $R_H$ ) was measured with the Van der Pauw method in Lake Shore 8400. Carrier concentration ( $n_H$ ) and carrier mobility ( $\mu_H$ ) were estimated by  $n_H = 1/(eR_H)$  and  $\mu_H = \sigma \cdot R_H$ , respectively.

**Electrical transport properties:** The Seebeck coefficient and electrical conductivity were measured by Cryoall CTA instrument under a helium atmosphere from room temperature to 800 K. The uncertainty of the Seebeck coefficient and electrical conductivity measurement is 5%.

**Thermal conductivity:** The thermal conductivity was calculated through  $\kappa = D \cdot C_P \cdot \rho$ , where  $D$ ,  $C_P$ ,  $\rho$  are thermal diffusivity, heat capacity and sample density, respectively. The thermal diffusivity ( $D$ ) was measured by the laser flash diffusivity method with Netzsch LFA 457, the heat capacity ( $C_P$ ) was estimated with the Dulong-Petit law, the sample density ( $\rho$ ) was calculated using the measured dimensions and weight. The combined uncertainty for all measurements involved in the calculation of  $ZT$  is around 20%.

**Differential scanning calorimeter (DSC) measurements:** The differential scanning calorimeter (DSC) measurements were performed on Netzsch STA 449 F3 simultaneous thermal analyzer in crucible under a N<sub>2</sub> flow, in the proper temperature range.

**Lorenz number calculations:** A single parabolic band (SPB) model with acoustic

---

phonon scattering was used to estimate Lorenz number ( $L$ ). Generally, Lorenz number can estimate the lattice thermal conductivity, which will not change the total thermal conductivity and final  $ZT$  values. The Lorenz number is given by the formula<sup>1</sup> :

$$L = \left( \frac{k_B}{e} \right)_2 \left( \frac{(r + 7/2)F_{r+5/2}(\eta)}{(r + 3/2)F_{r+1/2}(\eta)} - \left[ \frac{(r + 5/2)F_{r+3/2}(\eta)}{(r + 3/2)F_{r+1/2}(\eta)} \right]_2 \right) \quad (1)$$

where  $k_B$  is the Boltzmann constant and  $\eta$  is the reduced Fermi energy, which can be derived from the measured Seebeck coefficients *via* the following equations:

$$S = \pm \frac{k_B}{e} \left( \frac{(r + 5/2)F_{r+3/2}(\eta)}{(r + 3/2)F_{r+1/2}(\eta)} \right) \quad (2)$$

where  $F_n(\eta)$  is the nth order Fermi integral:

$$F_n(\eta) = \int_0^\infty \frac{x^n}{1 + e^{x-\eta}} dx \quad (3)$$

$$\eta = \frac{E_f}{k_B T} \quad (4)$$

Acoustic phonon scattering is the main carrier scattering mechanism, resulting in  $r$  value of -1/2.

**Cahill model calculations:** The theoretical minimum lattice thermal conductivity  $\kappa_{min}$  of a normal solid is calculated by Cahill's formula<sup>2</sup>:

$$\kappa_{min} = \left( \frac{\pi}{6} \right)^{\frac{1}{3}} \kappa_B n^{\frac{2}{3}} \sum_i^3 v_i \left( \frac{T}{\theta_i} \right)^2 \int_0^{\theta_i} \frac{x^3 e^x}{(e^x - 1)^2} dx \quad (5)$$

where  $k_B$  is the Boltzmann constant,  $n$  is the number density of atoms,  $v_i$  is the speed sound, and  $\theta_i (= v_i (\hbar / k_B) (6\pi^2 n)^{1/3})$  is the cut-off frequency for each polarization.

This model is taken over three sound modes including one longitudinal  $v_l$  and two transverse  $v_t$  branches. The longitudinal  $v_l$  and transverse speed sound  $v_t$  for each sample are measured, respectively. The obtained  $\kappa_{min} \sim 0.42 \text{ W m}^{-1} \text{ K}^{-1}$  of GeTe sample is shown in **Figure 6b** by a dashed line. Clearly, the measured  $\kappa_L$  of solid solution is close to  $\kappa_{min}$  especially in the high temperature range.

**Callaway model calculations:** Above Debye temperature, the ratio between the lattice thermal conductivity of multiple component samples (Ge<sub>0.88</sub>In<sub>0.02</sub>Pb<sub>0.1</sub>Te, Ge<sub>0.89</sub>In<sub>0.010</sub>Pb<sub>0.1</sub>Te<sub>0.997</sub>I<sub>0.003</sub>, Ge<sub>0.84</sub>In<sub>0.010</sub>Pb<sub>0.1</sub>Sb<sub>0.05</sub>Te<sub>0.997</sub>I<sub>0.003</sub>) and parent sample (

---

GeTe ) can be expressed as follows<sup>3, 4</sup>:

$$\frac{\kappa_{lat}}{\kappa_{lat,p}} = \frac{\tan^{-1} u}{u} \quad (6)$$

where  $\kappa_{lat}$  and  $\kappa_{lat,p}$  are lattice thermal conductivities of multiple component samples and parent sample, respectively. The parameter  $u$  is defined as follows<sup>5, 6</sup>:

$$u = \left( \frac{\pi^2 \theta_D \Omega}{h v_a^2} \kappa_{lat,p} \Gamma \right)^{\frac{1}{2}} \quad (7)$$

where  $h$  is the Planck constant,  $\Omega$  is the volume per atom,  $v_a$  is the average lattice sound velocity ( $v_a = 2055$  m/s).  $\Gamma$  is the imperfection-scaling parameter included mass fluctuation  $\Gamma_M$  and strain field fluctuation  $\Gamma_S$ . The relation between  $\Gamma_M$  and  $\Gamma_S$  can be written as  $\Gamma = \Gamma_M + \varepsilon \Gamma_S$ , where  $\Gamma_M$  is calculated by averaging sublattice mass,  $\Gamma_S$  is calculated by averaging sublattice ionic radius,  $\varepsilon$  is an adjustable parameter.  $\varepsilon = 2(W+6.4\gamma)^2$  is determined by the Grüneisen parameter  $\gamma=1.45$  and  $W=4$ <sup>7</sup>. Finally, we can obtain the theoretical predication  $\kappa_{lat}$  with Callaway model. The results are presented in **Figure 6c**.

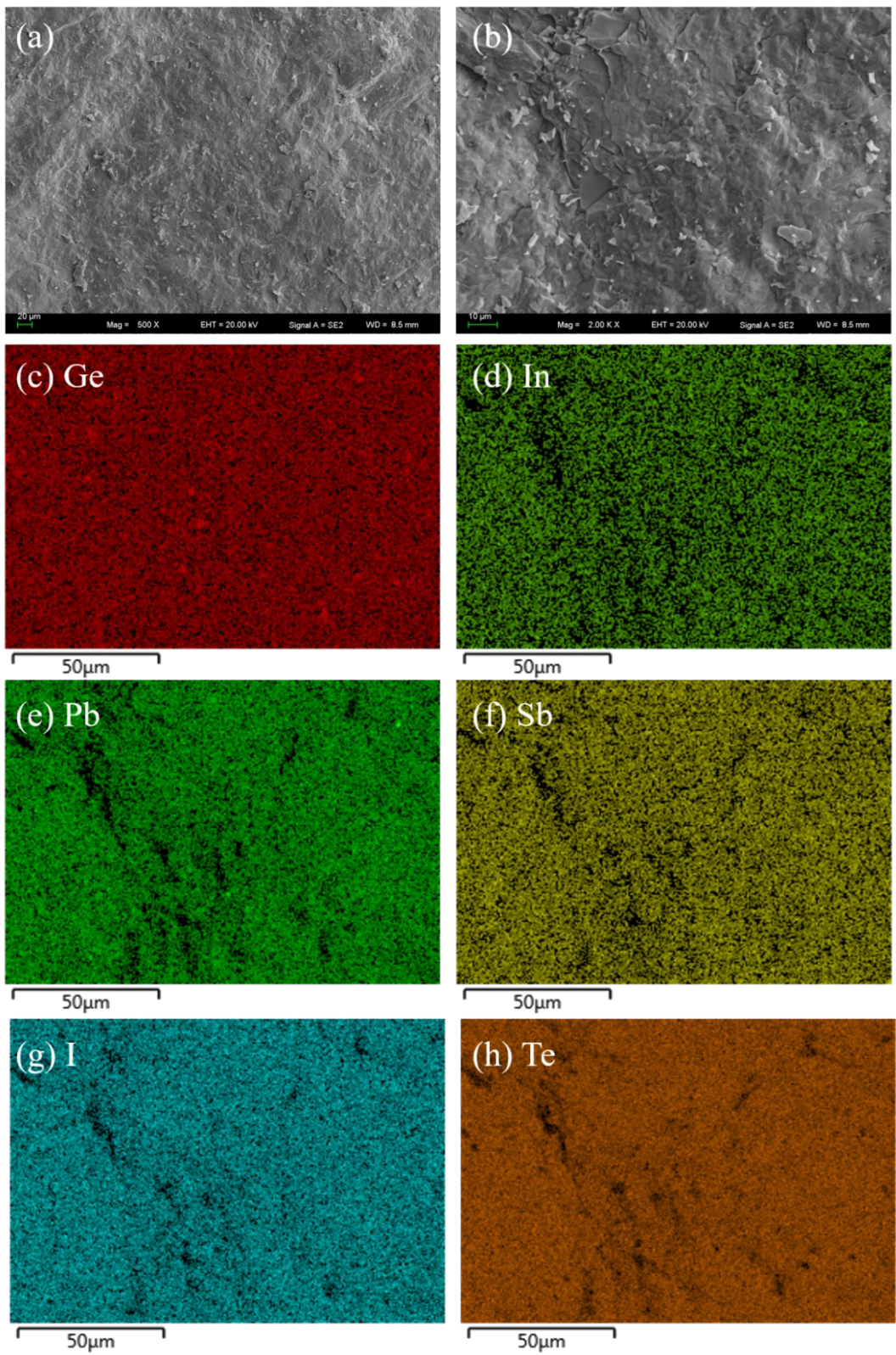


**Figure S1.** Secondary electron images for  $\text{Ge}_{0.84}\text{In}_{0.010}\text{Pb}_{0.1}\text{Sb}_{0.05}\text{Te}_{0.997}\text{I}_{0.003}$  (a) at low magnification and (b) at high magnification, respectively; Secondary X-ray maps in the selected area for (c) Ge element; (d) In element; (e) Pb element; (f) Sb element; (g) I element and (h) Te element.

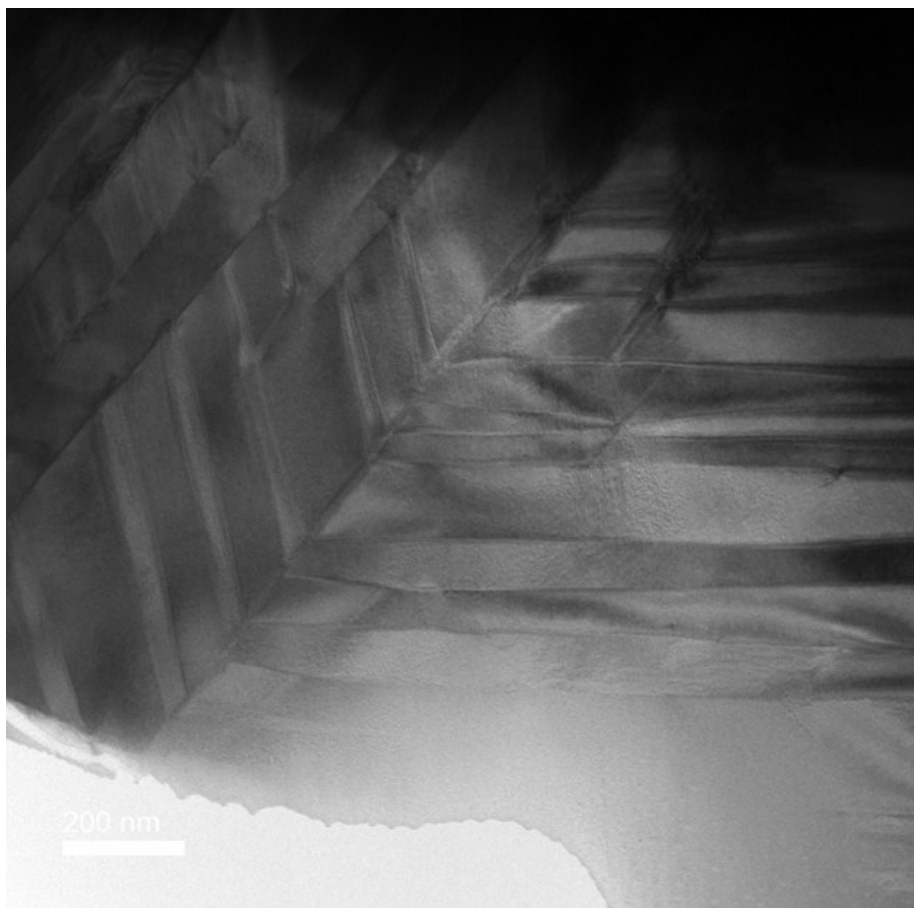


**Figure S2.** Low-magnification TEM images for  $\text{Ge}_{0.84}\text{In}_{0.010}\text{Pb}_{0.1}\text{Sb}_{0.05}\text{Te}_{0.997}\text{I}_{0.003}$ .

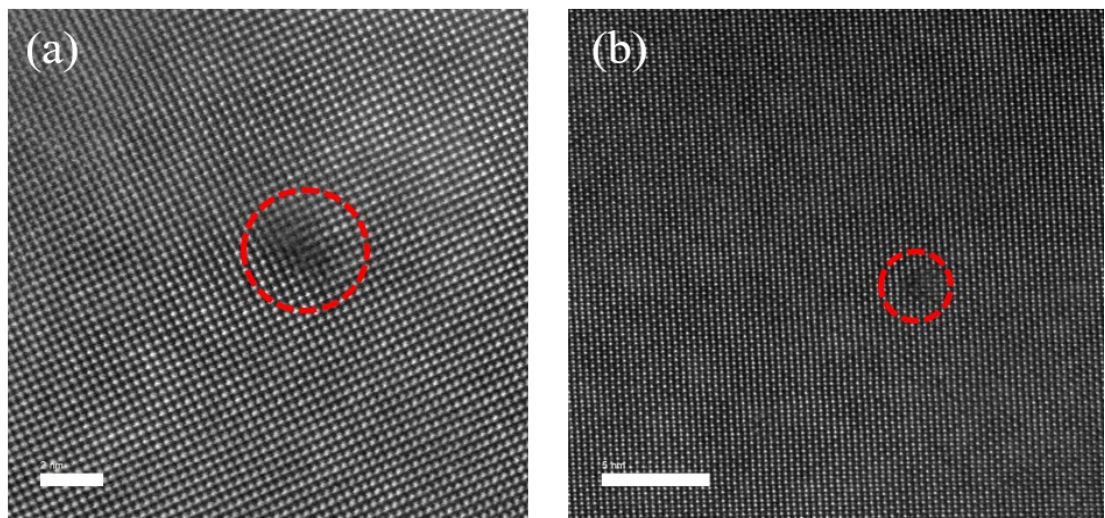


**Figure S3.** High-magnification STEM images taken along (a) [100] and (b) [001] zone axes of  $\text{Ge}_{0.84}\text{In}_{0.010}\text{Pb}_{0.1}\text{Sb}_{0.05}\text{Te}_{0.997}\text{I}_{0.003}$ .

---

## REFERENCES

1. L.-D. Zhao, S.-H. Lo, J. He, H. Li, K. Biswas, J. Androulakis, C.-I. Wu, T. P. Hogan, D.-Y. Chung, V. P. Dravid and M. G. Kanatzidis, *J. Am. Chem. Soc.*, 2011, **133**, 20476-20487.
2. D. G. Cahill, S. K. Watson and R. O. Pohl, *Physical Review B*, 1992, **46**, 6131-6140.
3. J. Yang, G. P. Meisner and L. Chen, *Appl. Phys. Lett.*, 2004, **85**, 1140-1142.
4. J. Callaway and H. C. von Baeyer, *Physical Review*, 1960, **120**, 1149-1154.
5. T. J. Gang, F. Shi, H. Sun, L. Zhao, C. Uher, V. Dravid and M. Kanatzidis, *J. Mater. Chem. A*, 2014, **2**, 20849-20854.
6. J. Li, X. Zhang, Z. Chen, S. Lin, W. Li, J. Shen, I. T. Witting, A. Faghaninia, Y. Chen, A. Jain, L. Chen, G. J. Snyder and Y. Pei, *Joule*, 2018, **2**, 976-987.
7. H. Wang, J. Wang, X. Cao and G. J. Snyder, *J. Mater. Chem. A*, 2014, **2**, 3169-3174.